PALLADIUM ISOTOPIC COMPOSITION OF IIAB and IVB IRON METEORITES. S. Sharma[1], M. Humayun[1], I. Leya[2] and Q-F. Mei[1]. [1]National High Magnetic Field Laboratory and Dept. Earth, Ocean & Atmospheric Science, Florida State University, Tallahassee, FL 32310, USA (ss18x@my.fsu.edu). [2]Space Research and Planetology, University of Bern, Bern, Switzerland.

Introduction: Nucleosynthetic isotopic anomalies indicating systematic s-process deficit in Mo, Ru and Pd isotopes have been observed for different meteorite groups [1-7]. Molybdenum isotopes have provided the most insight into these endemic nucleosynthetic anomalies, with two distinct groups: the carbonaceous meteorites (CC) and the non-carbonaceous meteorites (NC) recognized [8]. While both Ru and Pd isotopes have confirmed the presence of endemic anomalies in these elements, demonstration of an s-process deficit or the presence of distinct NC and CC groups has not yet been documented in either Ru or Pd isotopes, due to the difficulty of precisely measuring the p-process isotopes of Ru and Pd.

Palladium is a non-refractory, highly siderophile element with six naturally occurring stable isotopes—^{102}Pd, ^{104}Pd, ^{105}Pd, ^{106}Pd, ^{108}Pd, ^{110}Pd—with relative abundances of 1.02%, 11.14%, 22.33%, 27.33%, 26.46% and 11.72%, respectively. ^{102}Pd is a p-process isotope, ^{104}Pd is the s-only isotope, ^{105}Pd, ^{106}Pd, ^{108}Pd are produced by both s and r processes and ^{110}Pd is the r-process only isotope. An s-process deficit in Pd when normalized to ^{108}Pd/^{105}Pd will produce a negative ε^{104}Pd and ε^{106}Pd and a positive ε^{110}Pd. Palladium isotope studies of IVB irons found correlated excesses in ε^{110}Pd with deficits in ε^{104}Pd consistent with 0.005% s-deficit, about half the effect found in Mo isotopic composition, 0.01-0.15% [5]. This difference between Pd and Mo has been attributed to chemical processing of the presolar carriers of nucleosynthetic anomalies within the solar system. Complicating efforts to study nucleosynthetic anomalies in Pd is neutron capture of ^{103}Rh to form ^{104}Pd in iron meteorites.

In this study, we report the Pd isotope composition of IIAB and IVB irons. There is a cosmogenic effect associated with ε^{104}Pd. The neutron capture on ^{103}Rh produces ^{104}Pd- the absolute anomaly produced is a function of the Rh/Pd ratio and the exposure time. This cosmogenic dosimeter has been shown to be correlated with excesses in ^{192}Pt in IVB irons [5]. To better understand the neutron capture effects, we focused on a study of IIAB irons, the magmatic iron meteorite group with the largest range in elemental abundances due to fractional crystallization [9]. Combined Pd, W and Re isotopes were obtained on four IIABs spanning a broad range of Ir abundances.

Analytical Methodology: Five IVB iron meteorites: Skookum (Sk), Kokomo (Kk), Catalina 003 (C003), Dumont (Du) and Ternera; four IIAB irons: Carver (Ca), Richland (Ri), Sandia Mountains (SMt) and Sikhote Alin (SA) were analyzed for palladium isotopic composition using a Thermo Neptune™ MC-ICP-MS at the Plasma Analytical Facility, National High Field Magnetic Laboratory, Florida State Univer-sity. All samples were dissolved using aqua regia in Savillex™ PFA beakers at 150°C. Two-stage chemical separation using cation exchange column (removal of bulk matrix Fe, Ni, Zn, Ti etc.) and anion exchange columns was performed to obtain pure Pd aliquots with ^{101}Ru/^{105}Pd ratio better than $1x10^{-4}$.

The isotopic acquisition was done in low resolution and static mode for 5 blocks of 200 cycles each using up to 500 ng/mL Pd aliquots in 5% HCl introduced with a SIS glass spray chamber. The acquired raw ratios were corrected for mass bias with the exponential law normalized to ^{108}Pd/^{105}Pd = 1.18899 [10]. Palladium isotopic composition is reported in epsilon notation, i.e., deviation from the reference material, an Alfa Aesar® Specpure® Pd standard.

$$\varepsilon^{i}\text{Pd} = [(^{i}\text{Pd}/^{105}\text{Pd})_{\text{sample}}/(^{i}\text{Pd}/^{105}\text{Pd})_{\text{standard}}] \times 10^4$$

where, i = 104, 106, 108 & 110 for Pd.

All Pd aliquots were analyzed with Thermo Element 2™ ICP-MS to measure abundances of impurities (Zn, Zr, Ru, Cd etc.) prior to measurement on the MC-ICP-MS. While collecting Pd isotope compositions, isobaric interferences from Ru (^{101}Ru) and Cd (^{111}Cd) were simultaneously monitored on the MC-ICP-MS. Typical 2SE reproducibility for ε^{104}Pd, ε^{106}Pd, and ε^{110}Pd was ±0.05, ±0.02, and ±0.06 ε units, respectively. Due to the large Ru isobaric corrections required, ε^{102}Pd was not obtained at the present time.

Precise determination of the Rh/Pd ratio of the dissolved iron meteorite samples was done using Thermo Element XR™ in low resolution. The precision obtained on the ratios was better than 0.5% RSD for Rh/Pd ratio.

Results: Fig. 1 shows the isotopic composition of IVB irons analyzed in this study. The results are comparable to the reported values for the same group in previous studies [5]. We observe excesses in ε^{110}Pd, but no distinguishable anomalies in ε^{106}Pd. Fig. 2 shows the Pd isotopic composition of the analyzed IIAB irons, Carver, Richland, Sandia Mountains, and Sikhote Alin. The average composition of IIAB irons is 0.02 ± 0.05 for ε^{106}Pd and 0.25 ± 0.08 for ε^{110}Pd.

The anomalies in ε^{104}Pd shown in Figs. 1-2 include the cosmogenic contributions.

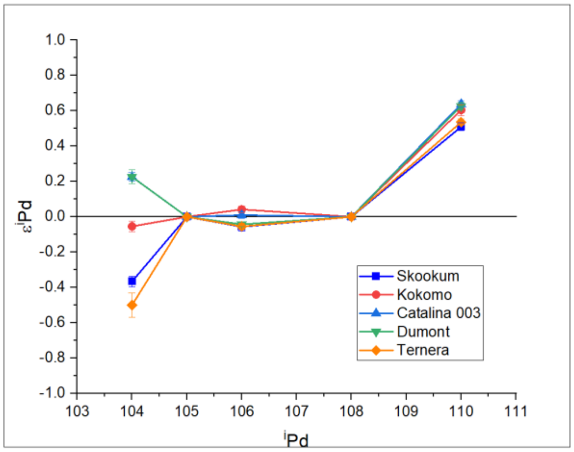

Fig. 1: Palladium isotopic composition of IVB iron meteorites analyzed in this study. Error bars are 2SE.

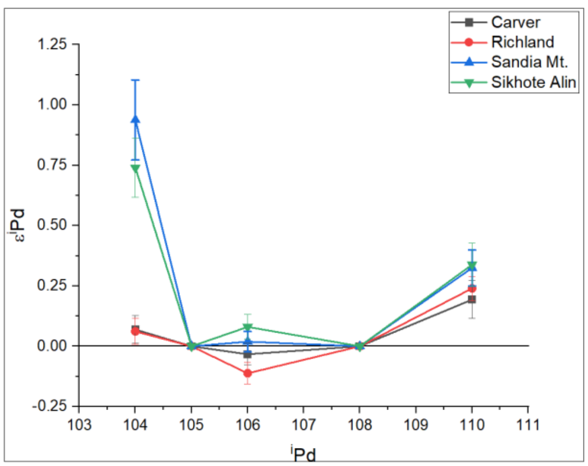

Fig. 2: Measured Pd isotopic composition of IIAB iron meteorites. ε^{104}Pd is not corrected for irradiation. Error bars are 2SE.

Discussion: The IIABs Sandia Mountains and Sikhote Alin show the largest cosmogenic effects. The Rh/Pd ratio of Sikhote Alin is greater than that of San-dia Mountain, but due to the shorter exposure age 430 Ma as compared to 720 Ma for Sandia Mountains [11], a smaller anomaly is observed.

We used the model developed by [12] to under-stand the effect of neutron capture in Pd isotopes. The model code requires the exposure age together with Rh/Pd as input to calculate the cosmogenic anomalies that would be produced as a result of neutron capture on ^{103}Rh. Fig. 3 plots the calculated e^{104}Pd with respect to Rh/Pd ratio for different exposure ages -100 Ma, 250 Ma, 500 Ma, 750 Ma and 1000 Ma. For any expo-sure age and Rh/Pd ratio, the calculated ε^{104}Pd ranges from 0 to the maximum as depth increases. The shaded contours show the range of ε^{104}Pd values that can be produced as the Rh/Pd ratio is varied for different ex-posure ages and size of the irradiated body. The shaded area with higher exposure age can produce all the val-ues ranging from 0 to the maximum at the contour end.

In Fig. 3, we observe a negative correlation be-tween ε^{104}Pd and Rh/Pd ratio for the analyzed samples. This figure is contoured by exposure age to show the effects of both Rh/Pd ratio and exposure age. Carver and Richland have the highest Rh/Pd ratios, but the smallest anomalies in ε^{104}Pd. It could be a reflection of the exposure ages or the exposure geometry of the samples. A small exposure age cannot produce highly anomalous ε^{104}Pd, even with appreciable Rh/Pd.

Another explanation is that the samples may not have been from enough within the irradiated meteor-oid. The production of cosmogenic neutrons peaks around 120 cm deep inside the body (for uniform irra-diation of a spherical iron) [12]. If the sample came from the exterior of the meteorite, then it will not show high ε^{104}Pd at any Rh/Pd or exposure age.

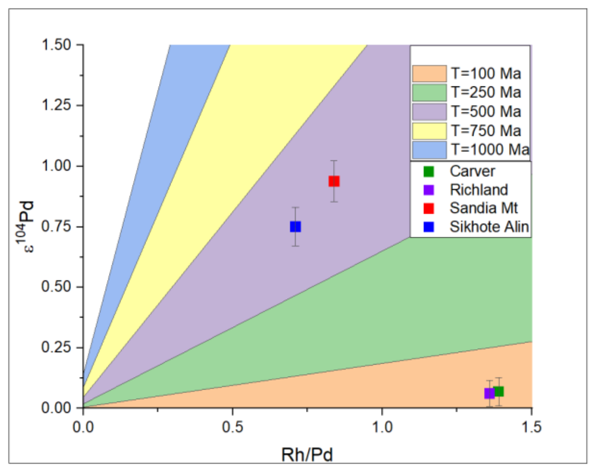

Fig. 3: A stacked area plot of ε^{104}Pd vs. Rh/Pd con-tours for different exposure ages generated using the model of [12]. The measured data for the analyzed IIAB irons is superimposed on the contours.

References: [1] Dauphas, N. et al. (2004) *EPSL*, 226, 465-475. [2] Chen, J. H., et al. (2010) *GCA*, 74, 3851-3862. [3] Burkhardt, C., et al. (2011) *EPSL*, 312, 390-400. [4] Bermingham, K. R., et al. (2018) *EPSL*, 487, 221–229. [5] Mayer B. et al. (2015) *ApJ*, 809, 180. [6] Budde G. et al. (2016) *EPSL 454*, 293-303. [7] Mayer B. and Humayun M. (2016) *LPSC 47*, Abstract # 2047. [8] Kruijer T. et al. (2017) *PNAS 114*, 6712-6716. [9] Wasson J. T. et al. (2007) *GCA 71*, 760-781. [10] Kelly, W. R. and Wasserburg, G. J. (1978) *GRL*, 5, 1079 [11] Voshage H. 1984, *EPSL*, 71, 181-194 [12] Leya I. and Masarik J. (2013) *MAPS, 48*, 665-685.